

Development a simple point source model for Elekta SL-25 linear accelerator using MCNP4C Monte Carlo code

A. Mesbahi*

Department of Medical Physics, Medical School, Tabriz University of Medical Sciences, Tabriz, Iran

Background: Monte Carlo (MC) modeling of a linear accelerator is a prerequisite for Monte Carlo dose calculations in external beam radiotherapy. In this study, a simple and efficient model was developed for Elekta SL-25 linear accelerator using MCNP4C Monte Carlo code. **Materials and Methods:** The head of Elekta SL-25 linac was simulated for 6 and 18 MV photon beams using MCNP4C MC code. Energy spectra and fluence distribution of photons crossing the phase space plane were calculated. A simple point source model was developed based on calculated photon spectra and spatial distribution. Using this model, percent depth doses (PDDs), and beam profiles were calculated for different field sizes. The results of MC calculations were compared with measurements. **Results:** There was a good agreement between MC calculations and measurement for descending part of PDD curves. However, comparing calculated PDDs with measurement showed up to 10% differences for build up region of PDD curves for both energies. For beam profiles, there was 2% difference in flat region and up to 15% difference was seen for out of field region. These results were acceptable according to the recommended criteria. Using this model, the run time was decreased 24 times in comparison to original full Monte Carlo method. **Conclusion:** Our study showed the presented model to be accurate and effective for MC calculations in radiotherapy treatment planning. Also, it substantially lowers MC runtime for radiotherapy purposes. *Iran. J. Radiat. Res., 2006; 4 (1): 7-14*

Keywords: Monte Carlo modeling, medical linear accelerator, MCNP4C, radiotherapy dose calculations.

INTRODUCTION

Monte Carlo (MC) method is the most accurate method for dose calculations in radiotherapy. It has been used in many applications including external photon and electron beam therapy, brachytherapy, etc. (1). MC method has overcome the deficiencies of analytical dose calculation methods in conditions such as tissue inhomogeneities and electronic disequilibrium with small fields(2-5).

For the application of MC calculations in external beam radiotherapy, a 2-step development approach is followed. The first step requires a realistic model of the linear accelerator or Cobalt-60 machine treatment head to quantify the energy, angular, and positional, distribution of photons and electrons entering the patient (6-10). This initial simulation is performed once and requires a reformat of the treatment head Phase-Space (PS) distribution into a virtual source model (9, 10). This virtual source must recreate the distribution of photons and electrons exiting the treatment head without the time-consuming process of simulating individual photon and electron trajectories through the various patient-independent structures of the accelerator treatment head, such as the flattening filter. The second step utilizes this virtual source to simulate the depth dose and profile characteristics incident upon a water phantom. A phase space file containing the energy, angular, and spatial distribution of photons and electrons crossing a plane normal to the beam central axis contains all particle information necessary for calculating the dose in a patient and the computer storage requirements can be quite large, requiring up to 1 Gigabyte of storage space. Bearing in mind that several beam qualities and a large number of field sizes are available per linac, the need to compress PS data becomes obvious.

Therefore, beam models were constructed(6-7). The feasibility of a beam model for radiotherapy treatment planning has to be

*Corresponding author:

Dr. Asghar Mesbahi, Department of Medical Physics, Medical School, Tabriz University of Medical Sciences, Tabriz, Iran.

Fax: +98 411 3364660

E-mail: asgharmesbahi@yahoo.com

demonstrated by calculating dose distributions and comparing them to measurements. Simple beam models are used as an effective and fast way to calculating dose distributions in irradiated medium^(2, 6). In a research by Fix *et al.* four simple models were developed using GEANT MC codes and their accuracy were evaluated against measurements. Their study showed that the simple model consisted of radially dependent energy spectra together with the spatial photon fluence distribution had reasonable accuracy for MC calculations⁽⁶⁾. In current work, the treatment head of Elekta SL-25 linac was simulated. The photon spectra for 6 and 18 MV photon beams were calculated using MCNP4C MC code. Also, a simple source model based on work of Fix *et al.* was developed in order to decrease the time of MC calculations in radiation therapy. The dosimetric characteristics of modeled linac was analyzed and compared to measurements.

MATERIALS AND METHODS

Monte Carlo modeling of Elekta SL 25 linac

The MCNP4C MC code is currently used to create and evaluate the phase space distributions from linear accelerator simulations⁽¹⁻⁵⁾. This code allows the development of detailed 3D models of a linear accelerator treatment head⁽¹¹⁾.

In this study, we simulated the head of Elekta SL-25 (Elekta oncology systems, Stockholm, Sweden) completely based on manufacturer's detailed information. The components of a linear accelerator for 6 and 18 MV photon beams are shown in figure 1. The wedge was not included in our simulations. Also, previous studies have shown that the monitor ionization chamber has not significant impact on photon beam characteristics^(7, 9). In study of Fix *et al.* (2001), the relative number of particles in photon beam from beryllium window and monitor ionization chamber has been about 1% for all field sizes. So, it was not simulated in our study. The model constructed to simulate the Elekta SL-25 linear accelerator head incorporated the major

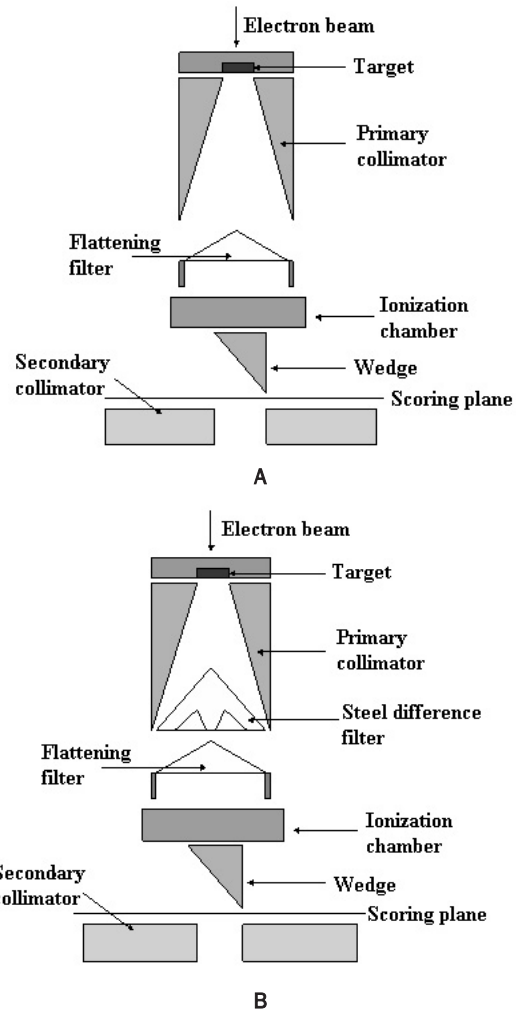


Figure 1. The schematic representation of Elekta 25 SL Linac head geometry used for simulation of (A) 6 MV and (B) 18 MV photon beams. In our simulation, the ionization chamber and the wedge were not included.

components in the beam path. The target comprised 3 mm thick tungsten (95%), nickel (3.75%) and iron (1.25%) alloy of density 18.0 g/cm³, attached to a 4.5 mm thick copper backing plate. The incident electron beam striking the target was simulated by a spot size of 1 mm full width half maximum (FWHM) with at the nominal accelerating potential of 6 and 18 MeV. Immediately under the target is the primary conical collimator comprising a 28° cone bored in a metal (lead 96% and antimony 4%, density 11.12 g/cm³) block. The flattening filter is designed to differentially absorb the radiation and reduce the dose rate at the beam center; thus, the natural concentration of X-rays around the

direction of the electron stream and the rapid falling off to either side are corrected. It also acts as a radiation filter in the more traditional sense, i.e., by differential X-ray energy absorption it can change the radiation spectrum. The flattening filter for each energy was simulated according to the geometry drawings provided by manufacturer. For 18 MV beam a differential filter was added to 6 MV filter to create desired radiation intensity across the beam.

The Elekta SL-25 linear accelerator has a double plane adjustable diaphragm system providing secondary collimation and this was the final component to be modeled. The collimating face of each diaphragm (composition: lead 96% and antimony 4%) moves in such a way that it always lies along the direction of propagation of the radiation, i.e. along a radius from the source. In the model the collimating faces were arranged likewise. The simulation modeled the secondary collimators as having upper and lower jaws at different distances from the target (i.e. the mid depth point of the upper and lower collimators is 34 cm and 45 cm respectively from the target).

We developed a complete model of linac with above-mentioned components. Then, a water phantom with dimension of $30 \times 30 \times 30$ cm³ was simulated under treatment head with source-surface distance (SSD) of 100 cm and secondary collimators was set to create a field size of 10×10 cm² on phantom surface.

The exact mean energy of the electron beam incident on target is typically unknown and must be obtained by calibrating each spectral distribution against the corresponding depth dose curve by a trial-and-error method by choosing a suitable mean electron energy exiting the flight tube. Primary electron beam energies of both photon beams were determined by calculation of percent depth doses (PDD) for different energies of primary electron beams. For both beams, the percentage depth doses (PDDs) for 10×10 cm² field size were calculated. The range of primary electron energy was 6-6.5 MeV for 6 MV photons and 17.8-18.3 MeV for 18 MV. By comparing

calculated PDD with measurements, the primary electron energy for 6 and 18 MV photons were determined 6.4 and 18 MeV respectively. To obtain the statistical uncertainty less than 1% in our results, the runtime for PDD calculations in water phantom was about 1200 minutes.

After basic simulation for primary electron energy determination, we developed a model based on photon beam features that were obtained through our basic simulations. We applied simple virtual source model for our linac (6, 12). This model utilizes a two-step approach for simulating the depth dose characteristics from a linear accelerator. The first step requires a detailed simulation of the linac treatment head. This part of the simulation is calculated only once, since for a given energy, the geometry remains constant. The calculated bremsstrahlung spectra, differential in energy, angle, and position are used in the second step to simulate the depth dose and profile characteristics of the machine. Because the field size changes with each individual patient, this method simulates the movable jaws with the depth dose calculations.

To calculate the required data for developing virtual model, using the chosen initial electron energy, the bremsstrahlung phase space was scored at a point 35 cm downstream from the target and above the secondary collimators. This consisted of tallying the energy, angular, and spatial distribution of the bremsstrahlung spectra between the monitor chamber and the upper surface of secondary collimator. The MCNP4C next event estimator ring detector was used to tally the bremsstrahlung energy distribution. Each ring was positioned as a function of the subtended angle from the target in 1° increments from 0° to 9° (figure 2). This produced a simulated detector array that calculates the photon fluence, differential in energy and position. For each annular region the number of X-rays within 150 keV energy intervals crossing the scoring plane is recorded. A photon source is modeled as a modified point source whose location was defined by the SSD of the 100 cm. The

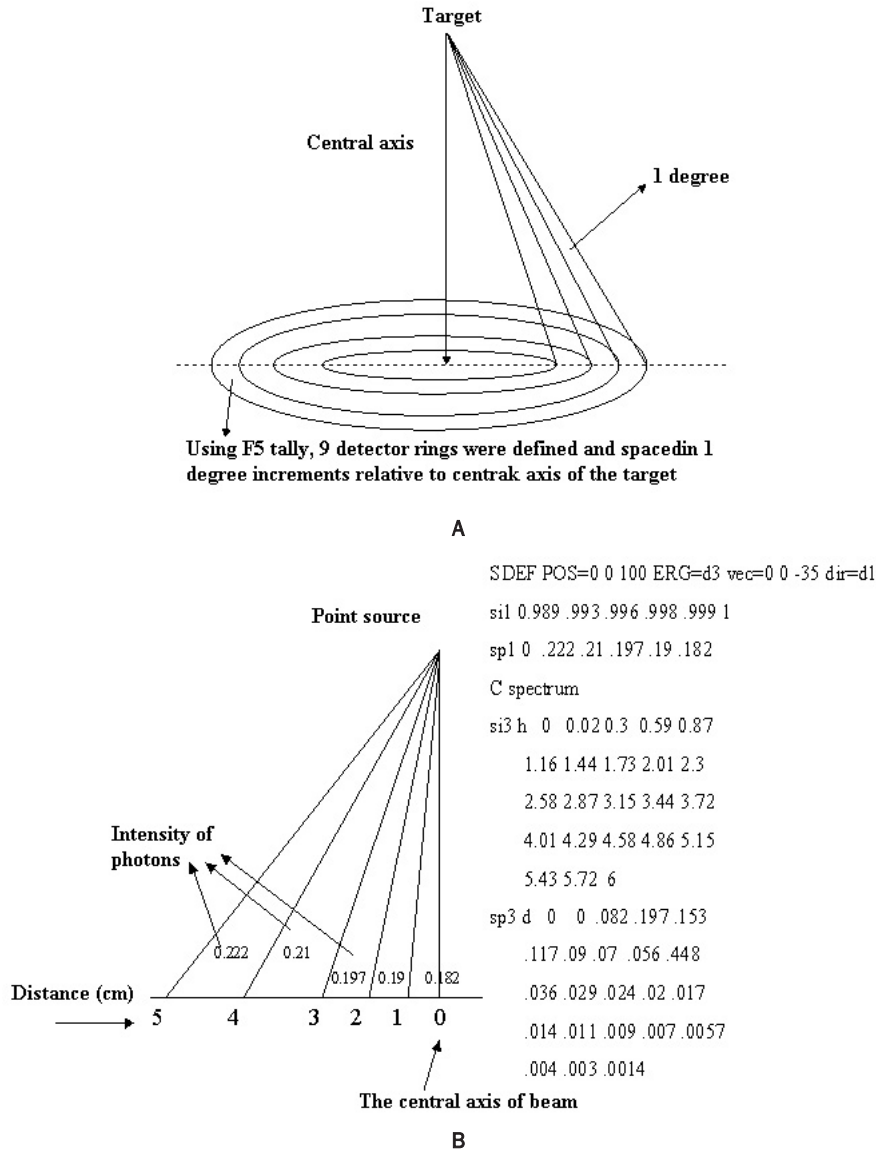


Figure 2. (A) Setup of detectors for scoring the photon fluence, differentiated in energy, angle and intensity. The detector tally plane was located 35 cm downstream from the front surface of the target. (B) This figure illustrates the definition of point source based on calculated photon beam spectra characteristics using ring detectors which is shown in figure (A). The numbers on the right side of part B show a brief definition of source in input file of MCNP4C.

MCNP4C point source allows the user to sample for energy and polar angle. The angular distribution is sampled as the cosine of the polar angle (μ) with an intensity weighting based upon the integrated photon fluence for each radial tally ring (figure 2B). Using this new model, the PDDs and beam profiles were calculated in a water phantom for different field sizes and then we compared them with measurements for validation of our MC model. Dose measurements were carried out by Scanditronix automatic water

phantom (RFA-300, Scanditronix Wellhofer AB, Sweden) and an ionization chamber (RK, Scanditronix Wellhofer AB, Sweden) with 0.125 cm³ volume. Measured results corrected for measurement point displacement of 1mm toward the phantom surface. PDDs for 5×5, 10×10, 20×20 and 30×30 cm² field sizes and beam profiles for the same field sizes at 10 cm depth were calculated using MC method and compared with measurements. All calculations were performed by a dual CPU desktop composed of two 2.3 GHz Athelon

processors. For our new model, the average run-time was between 45-60 minutes for calculation of PDDs for 10×10 cm² field size.

For depth dose calculations in water phantom, a cylinder with radius of one-tenth the size of the open field size was defined and divided into scoring cells with 2 mm height along the beam central axis. The simulation setup for beam profile calculations was identical to the depth dose calculations, except the primary cylinder was located at 10 cm depth vertically to beam central axis. The radius of cylinder was 2 mm. The dose resolution for depth dose and beam profile was 2 mm. The photon and electron low-energy cutoff were 10 and 500 keV respectively. The *F8 tally was used for dose calculations in water phantom. For all MC calculations the statistical uncertainty of results was less than 1% at d_{max} . The number of primary photons used for acquiring this statistical uncertainty was 5×10^8 .

RESULTS AND DISCUSSION

Water phantom benchmarks

Percentage depth dose curves for both energies and different field sizes were calculated and compared with measurements. The PDD curves and beam profiles for both energies are shown in figures 3-B and 4-B. In both figures, each beam profile was normalized to its maximum value in central axis and has been scaled for inclusion on the same graph. All depth dose curves were normalized to d_{max} and have been scaled for inclusion on the same graph. The statistical uncertainty of our Monte Carlo results was less than 1% for all depths.

Beam profiles for the different field sizes at the depth of 10 cm were calculated and compared by measurements. Figures 3-A and 4-A illustrate the comparison between MCNP4C profile calculations and water phantom measurements for both beam energies. There are several recommendations for evaluating dose calculation models performance in different situations, including homogenous simple geometry and complex

geometry (12, 13). Venselaar *et al.* (2001) recommended different criteria for the acceptance of calculation results in the water phantom. Their proposed values of tolerances for beam profiles are as follows: 1) umbra region, 2%; 2) penumbra region, 10%; 3) outside beam edge, 30%.

Due to the results, for off-axis points within the 50%-100% isodose range, the differences up to 3% can be observed. In the penumbra tail region, 10%-20% isodose level, MCNP4C underestimated the dose profiles by as much as 20%. The great local difference in this region also was reported for other MC codes by other investigators (2, 5, 6, 8-10); however, this difference is at out of field

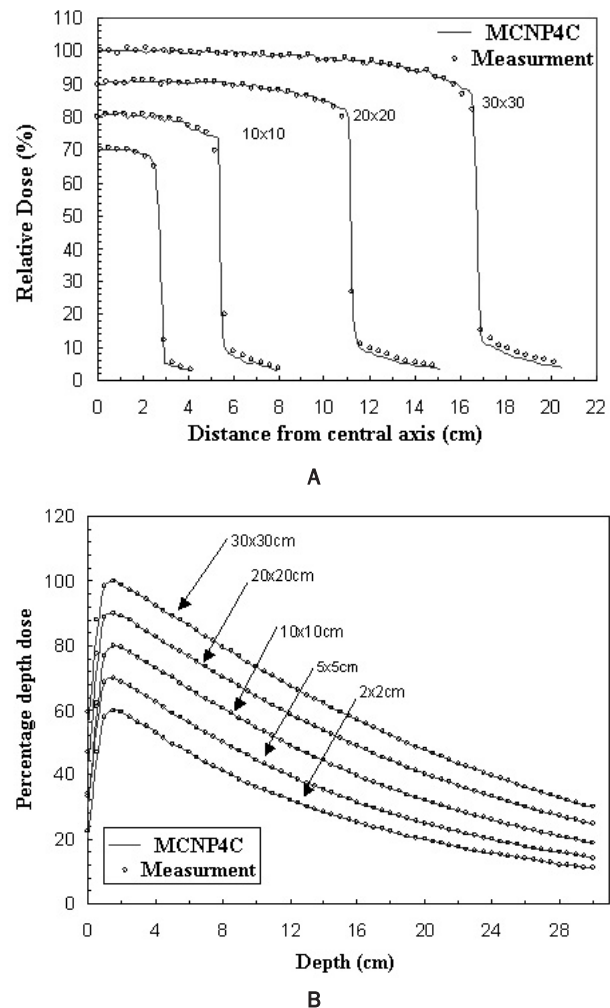


Figure 3. (A) Comparison of the MCNP4C beam profile calculations versus water phantom measurements for 6 MV photon beam at 10 cm depth. (B) Comparison of MCNP4C depth dose calculations versus water phantom measurements for 6 MV photon beam.

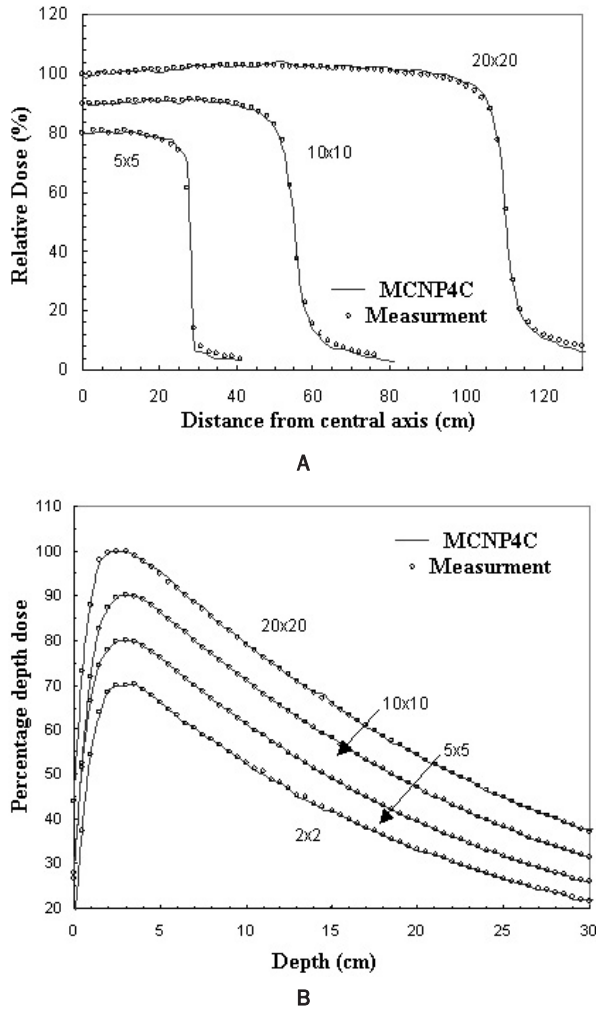


Figure 4. (A) Comparison of the MCNP4C profile calculations versus water phantom measurements for 18 MV photon beam at 10 cm depth. (B) Comparison of MCNP4C depth dose calculations versus water phantom measurements for 18 MV photon beam.

region, which is delivered by scattered radiations and does not affect our results in central axis of the beam. Also, according to the recommended criteria for this region if we normalize the differences to maximum value in beam profiles the differences will be within acceptable value of 3% (12).

There was a good agreement for MCNP4C calculations versus measurements in all parts of the depth dose curve including build-up region. The difference between measurements and MC calculations was less than 1.5% for descending part of PDD curves for both energies. But for build-up region, it reached up to 15% near the surface of phantom for 30x30 cm² field sizes in 18 MV beam.

According to Verhaegen and Seuntjens (2003), local differences less than 2% between measurements and calculations in PDD values are acceptable for model validation. However, the tolerance level for build up region has been higher due to several reasons. For homogenous and simple geometry (without wedge, inhomogeneity and asymmetry) the tolerance level of less than 10% has been recommended (12). In the build up region, the measurements with the ionization chamber are not completely reliable. This may be due to averaging effect of the chamber-sensitive volume in this high dose gradient region. On the other hand, it is well documented that MC dose calculations do not match well at narrow depths (8, 9). Siantar *et al.* (2001) have increased the dose contribution of the beam contaminant electrons in the Peregrine treatment planning system, in order to obtain good agreement between the MC calculated and measurement dose distributions at narrow depths.

Photon spectra at scoring plane

Photon energy spectra for 6 and 18 MV beams were calculated by ring detectors located 35 cm from the target. Figures 5 and 6 show the photon energy spectra for 6 and 18 MV photon beams which tallied by a ring detector subtends the angle of 1°. For both energies there was a peak on spectra, which belonged to annihilation photons of 511 keV energy. Two electron particles generated through the pair production effect interact

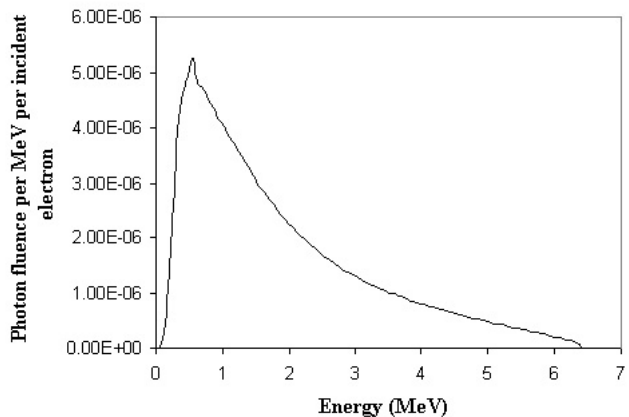


Figure 5. Photon energy spectrum for 6 MV beam calculated by a ring detector, which subtends 1° at 35 cm from target.

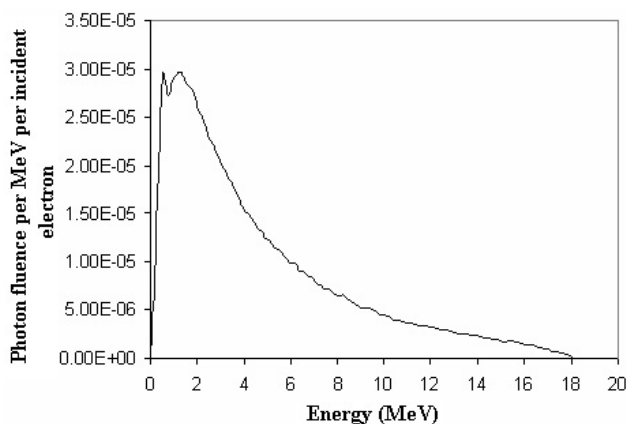


Figure 6. Photon energy spectrum for 18 MV beam calculated by a ring detector, which subtends 1° at 35 cm from target.

with each other and two annihilation photons were created.

The fluence of photons crossing ring detectors is shown in figure 7 for both energies. The intensity of photons in each angle relative to central axis of beam increases with distance from the center of

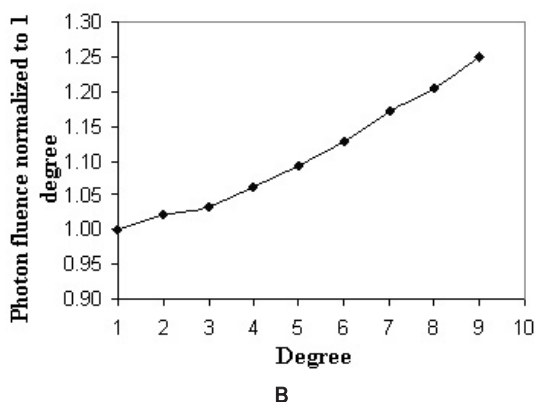
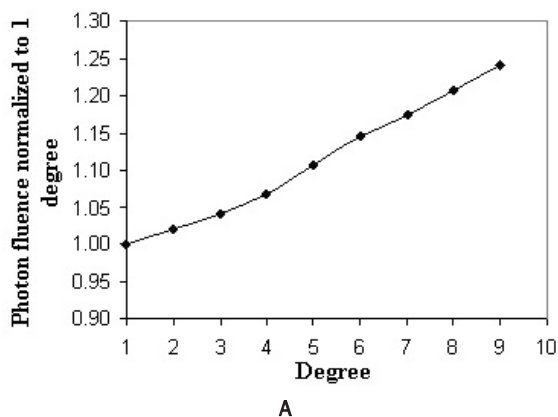


Figure 7. Radial dependence of fluence for photons crossing the scoring plane. The scoring ring detectors with different radius located at 35 cm from the target. (A) 6 MV beam. (B) 18 MV beam.

beam and becomes 25% higher in 9-degree relative to the intensity of photons for 1-degree detector for both energies. It can be seen that with increasing the radius of ring detector, the number of photons increases. This is because more low energy photons pass through the thinner lateral part of flattening filter and reach to the detector. Flattening filter used to reduce the intensity in the central part of the bremsstrahlung beam to reach an approximately constant energy fluence and flat dose profile across the beam in a specific depth of water. Consequently, the energy spectrum was harder on the beam central axis and becomes softer with distance from central axis.

CONCLUSION

To obtain accurate results from Monte Carlo simulations in radiotherapy calculations, precise modeling of Linac head and a sufficiently large number of particles are required. In this study we simulated Elekta SL-25 Linac based on manufacturer's information. We proposed a simple beam model to reduce runtime and statistical uncertainty in MC dose calculations in radiotherapy. We also commissioned calculation results for percentage depth dose curves and beam profiles for different field sizes using recommended criteria for photon beam models. Our results were in good agreement with recommended criteria for dose calculation in radiotherapy (12). Our simple model reduced the MC dose calculations 24 times in comparison to original MC model.

REFERENCES

1. Solberg TD, DeMarco JJ, Chetty IJ, Mesa AV, Cagnon CH, Li AN, Mather KK, Medin PM, Arellano AR, Smathers JB (2001) A review of radiation dosimetry application using the MCNP Monte Carlo code. *Radiochim Acta*, **89**: 337-355.
2. Demarco JJ and Solberg TD (1998) A CT-based Monte Carlo tool for dosimetry planning and analysis. *Med Phys*,

A. Mesbahi

- 25: 1-11.**
- Mesbahi A, Allahverdi M, Gharaati H (2005) Monte Carlo dose calculations in conventional thorax fields for ^{60}Co photons. *Radiat Med*, **23**: 341-350.
 - Ma CM, Pawlicki T, Jiang SB et al. (2000) Monte Carlo verification of IMRT dose distributions from a commercial treatment planning optimization system. *Phys Med Biol*, **45**: 2483-2495.
 - Mesbahi A, Thwaites D, Reilly A (2006) Experimental and Monte Carlo evaluation of Eclipse treatment planning system for lung dose calculations. *Rep Pract Oncol Radiother*, **11**: 1-11.
 - Fix MK, Keller H, Born EJ, Rügsegger P (2000) Simple beam models for Monte Carlo photon dose calculations in radiotherapy. *Med Phys*, **27**: 2739-2747.
 - Fix MK, Stampanoni M, Keller H, Born EJ, Mini R, Rügsegger P (2001) A multiple Source Model for 6 MV photon beam dose calculations using Monte Carlo. *Phys Med Biol*, **46**: 1407-1427.
 - Mesbahi A, Reilly A, Thwaites D (2006) Development and commissioning of a Monte Carlo Photon beam model for Varian CL 2100EX linear accelerator. *Appl Radiat and Isot*, **64**: 656-662.
 - Verhaegen F and Seuntjens J (2003) Monte Carlo modeling of external radiotherapy photon beams. *Phys Med Biol*, **48**: R107-R164.
 - Mesbahi A, Fix M, Allahverdi M, Grein E, Garaati H (2005) Monte Carlo calculation of Varian 2300C/D Linac photon beam characteristics: a comparison between MCNP4C, GEANT3 and measurements. *Appl Radiat and Isot*, **62**: 469-477.
 - Briesmeister JF (2000) MCNP-A general Monte Carlo N-particle transport code, Version 4C. Report LA-13709-M. Los Alamos National Laboratory, NM, USA.
 - Venselaar J, Welleweerd H, Mijneer B (2001) Tolerances for the accuracy of photon beam dose calculations of treatment planning systems. *Radiother Oncol*, **60**: 191-201.
 - Hartmann Siantar CL, Walling RS, Daly TP et al. (2001) Description and dosimetric verification of the PEREGRINE Monte Carlo dose calculation system for photon beams incident on a water phantom. *Med Phys*, **28**: 1322-1337.